Quasifree bremsstrahlung in the $dp \rightarrow dp\gamma$ reaction above the pion production threshold

J. Greiff,[1,*] I. Koch,[1] W. Scobel,[1] H. Rohdjeß,[2] J. Dyring,[3] K. Fransson,[3] L. Gustafsson,[3] S. Häggström,[3] B. Höistad,[3]
J. Johanson,[3] A. Johansson,[3] T. Johansson,[3] A. Khoukaz,[3] S. Kullander,[3] R. J. M. Y. Ruber,[3] J. Złomańczuk,[3] V. Dunin,[4]
B. Morosov,[4] A. Sukhanov,[4] A. Zernov,[4] J. Stepaniak,[5] R. Bilger,[6] W. Brodowski,[6] H. Clement,[6] G. J. Wagner,[6]
H. Calén,[7] C. Ekström,[7] A. Kupść,[7] P. Marciniewski,[7] J. Zabierowski,[8] B. Shwartz,[9] A. Sukhanov,[9] W. Oelert,[10] T. Sefzick,[10]
and A. Turowiecki[11]

[1]*I. Institut für Experimentalphysik, Universität Hamburg, D-22761 Hamburg, Germany*
[2]*Institut für Strahlen und Kernphysik, Universität Bonn, D-53115 Bonn, Germany*
[3]*Department of Radiation Sciences, Uppsala University, S-75121 Uppsala, Sweden*
[4]*Joint Institute for Nuclear Research, Dubna, 101000 Moscow, Russia*
[5]*Soltan Institute for Nuclear Studies, PL-00681 Warsaw, Poland*
[6]*Physikalisches Institut, Universität Tübingen, D-72076 Tübingen, Germany*
[7]*The Svedberg Laboratory, S-75121 Uppsala, Sweden*
[8]*Soltan Institute for Nuclear Studies, PL-90137 Lódź, Poland*
[9]*Budker Institute of Nuclear Physics, Novosibirsk 630090, Russia*
[10]*IKP, Forschungszentrum Jülich GmbH, D-52425 Jülich, Germany*
[11]*Institute of Experimental Physics, Warsaw University, PL-0061 Warsaw, Poland*

Experimental results of the $dp \rightarrow dp\gamma$ reaction are presented for several observables with deuteron projectile energies between 437 MeV and 559 MeV. The kinematically complete measurements were performed at the CELSIUS storage ring with the PROMICE/WASA setup. Angular and spectral distributions of the charged ejectiles are decomposed into fractions that can be attributed to a quasifree $np \rightarrow d\gamma$ process with a spectator proton and to a process involving all three nucleons. Within the acceptance of the detector, about two thirds of the events are associated to the quasifree process; the remainder are characterized by substantial transverse momentum components transferred to a participating outgoing proton.

I. INTRODUCTION

Bremsstrahlung from nucleus-nucleus and from proton-nucleus interactions show characteristics suggesting that the main source of the γ emission are primarily the nucleon-nucleon scattering processes $NN \rightarrow NN\gamma$ [1], where N denotes either a proton p or a neutron n. Consequently, $NN \rightarrow NN\gamma$ is an essential ingredient for models of the bremsstrahlung process on nuclei, that will, however, be influenced by the presence of additional nucleons. This impact of the nuclear environment on the inelastic NN interaction may be studied by a comparison of the photon production in pd interaction to the free two nucleon processes $pn \rightarrow pn\gamma$, $pn \rightarrow d\gamma$, and $pp \rightarrow pp\gamma$.

Possible reaction mechanisms may be grouped into the following classes [2]: (1) $pd \rightarrow {}^3\mathrm{He}\gamma$, (2a) $pd \rightarrow pn\gamma p_s$, (2b) $pd \rightarrow pp\gamma n_s$, (2c) $pd \rightarrow pnp\gamma$, (3a) $pd \rightarrow d\gamma p_s$, (3b) $pd \rightarrow pd\gamma$.

For the radiative capture mechanism (1), we refer to Ref. [3]. The mechanisms (2a) and (2b) are genuine quasifree $NN \rightarrow NN\gamma$ processes where one of the nucleons of the target deuteron enters only as spectator N_s. When compared to the free two-nucleon case, the folding with the momentum distribution of the participating target nucleon will extend the

photon spectrum to higher energies. This approach was followed by Nakayama [4] based upon mechanism (2a) only, since mechanism (2b) is expected to play a minor role [5] due to the smaller elementary cross sections for $pp \rightarrow pp\gamma$ as compared to $pn \rightarrow pn\gamma$. Finally, mechanism (2c) represents all processes involving all three nucleons.

The processes (3a) and (3b) are more complex. They include:

(3a) pn bremsstrahlung as in mechanism (2a) with p_s and a momentum match between the interacting nucleons that leads to a deuteron bound state [Fig. 1(a)]. This is also called a quasifree (QF) radiative capture in the np system.

(3b) The coherent bremsstrahlung on the deuteron. We use this term as a synonym for all reactions involving all three nucleons. This includes processes where the deuteron is considered as a fundamental particle as well as those where the γ is produced in $pN \rightarrow pN\gamma$ interactions [Fig. 1(b)] or in $pn \rightarrow d\gamma$ after initial pN scattering [Fig. 1(c)] or more complex processes not shown here.

So far comprehensive theoretical calculations for $pd \rightarrow pd\gamma$, including several of the processes listed above are not available.

Nakayama [4] uses a meson-exchange potential for the elementary pn bremsstrahlung amplitude to describe pd bremsstrahlung. He obtains at most a qualitative agreement with then existing inclusive experimental $pd \rightarrow X\gamma$ data [5,6]. In particular, it was necessary to multiply the predicted values with an arbitrary normalization factor of 1.67 to achieve agreement with the experimental data, indicating
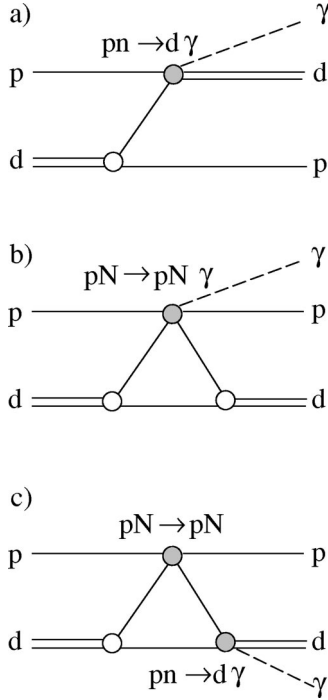
FIG. 1. Diagrams for some possible $dp \rightarrow dp\gamma$ production mechanisms: (a) quasifree production mechanism via $pn \rightarrow d\gamma$, also called spectator model; (b) and (c) so called coherent mechanisms, (b) includes quasifree production via $pN \rightarrow pN\gamma$, (c) includes rescattering.

that important contributions to the total pd bremsstrahlung cross section were not understood.

More recently Huisman *et al.* [7] have studied the $pp \rightarrow pp\gamma$ reaction, both experimentally and with microscopic model calculations, concluding that at present no high-quality NN model calculation consistent with $pp \rightarrow pp\gamma$ data exists. It must be suspected that this applies more to calculations for $pd \rightarrow pd\gamma$, owing to the increased complexity. To this end exclusive data on $pd \rightarrow pd\gamma$ is needed, in order to select kinematic regions where only one or a few of the reaction channels are believed to be dominant. Then the interpretation of the data should be easier. Particularly, good reaction mechanisms to study are those involving a spectator nucleon.

Experimentally, there is still a lack of high-quality bremsstrahlung data in the pd system. From here on we denote the initial state with the first particle being the projectile and the second the target, i.e., pd a proton beam impinging on a deuteron target, and dp the process with inverse kinematics.

First experiments were carried out in the late 1960s. Edington *et al.* [8] have measured the inclusive $pd \rightarrow X\gamma$ reaction at $T_p = 145$ MeV and Koehler *et al.* [2] at $T_p = 197$ MeV with contradicting results concerning the total cross sections as well as the importance of different production mechanisms. Later Pinston *et al.* [5] presented results for $pd \rightarrow X\gamma$ at $T_p = 200$ MeV, and Clayton *et al.* [6] at $T_p = 145$ and 195 MeV, both in agreement with the results from Ref. [2].

None of these experiments were able to distinguish between the different reaction channels mentioned above be-

cause they only measured the outgoing γ. The energy range under study was also limited by the π^0-production threshold because of the difficulties to reject events with γ's originating from π^0 decays.

The experimental situation is different for the radiative capture channel $pd \rightarrow {}^3\text{He}\gamma$, which can be more easily separated due to the constraints that can be applied for binary reactions. Several exclusive measurements exist for $pd \rightarrow {}^3\text{He}\gamma$ and the inverse radiative capture process $\gamma{}^3\text{He} \rightarrow pd$ (see e.g., [9,10,3] and references therein).

Preliminary results have recently been presented for pd bremsstrahlung at $T_p = 190$ MeV [11]. In addition to the γ the charged ejectiles were also detected, but not identified. Therefore, this experiment might yield exclusive results beyond $pd \rightarrow {}^3\text{He}\gamma$.

The most straightforward way to improve the database for pd bremsstrahlung experimentally is to investigate it with a detector setup capable not only to detect γ's, but also to measure and identify all the outgoing charged particles with a good acceptance.

The reaction channels (2a) and (3a) have the inherent experimental difficulty that the spectator protons are emitted with small momenta in the initial deuteron rest frame. Their direct detection in pd reactions requires the measurement of low energy spectator protons. For this purpose the detector has to be placed around the vertex *inside* the target chambers since even thin target chamber windows absorb most of the spectator protons (see e.g., Ref. [12]). This difficulty can be overcome by using *deuteron projectiles* in conjunction with *hydrogen targets* to boost the energy of the spectator nucleons [13].

The experiment presented here follows this line and is the first exclusive measurement of a spectator mechanism $dp \rightarrow d\gamma p_s$ above the pion production threshold.

The paper is organized as follows. Section II gives a description of the detector, the measurements, and the event selection procedure. In Sec. III, we discuss the reaction models for $dp \rightarrow dp\gamma$ used in the Monte Carlo simulation, and in Sec. IV we compare the experimental results with the simulations and present total cross sections for $dp \rightarrow d\gamma p_s$. The conclusions are summarized in Sec. V.

II. EXPERIMENTAL SETUP AND MEASUREMENTS

A. General

The experiment has been performed at the cooler synchrotron CELSIUS of the The Svedberg Laboratory [14] with a deuteron beam impinging on an internal hydrogen cluster jet target. The experiment mainly aimed at the investigation of the production mechanism for $dp \rightarrow dp\pi^0$ for which the results are given in Ref. [13]. Measurements were carried out at five different projectile energies between $T_d = 437$ and 559 MeV (The threshold for $dp \rightarrow dp\pi^0$ is 414.5 MeV.) Two production runs were separated by half a year and the lowest projectile energy was repeated for a consistency check.

The CELSIUS storage ring was filled with typically 2×10^9 deuterons by stripping injection. Electron cooling was applied at the two lowest energies $T_d = 437$ MeV and 454
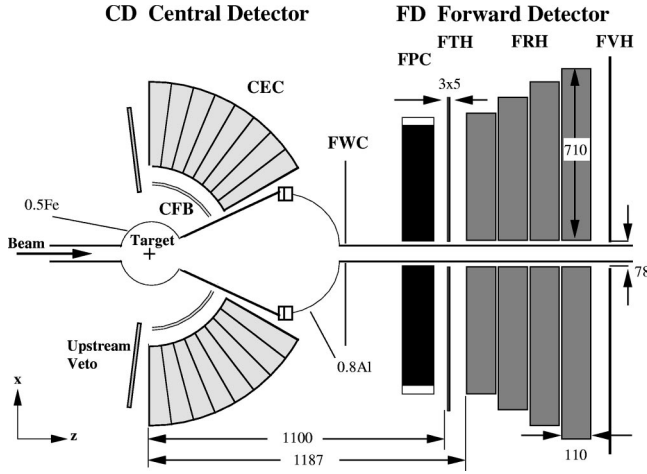
FIG. 2. PROMICE/WASA detector at the CELSIUS storage ring (dimensions are given in mm).

MeV to improve the signal-to-background ratio for these runs.

B. Target and PROMICE/WASA detector

The experiment used the PROMICE/WASA setup and is shown schematically in Fig. 2. It can be divided into the target system, the central detector (CD) for photon and charged particle detection, and the forward detector (FD) section for charged particles.

The target was operated with pressurized H_2 gas that was vertically injected into the interaction region through a nozzle cooled to 20–30 K [15]. At the intersection with the CELSIUS beam the jet formed a beam of 6.5 mm diameter across and 10.5 mm along the direction of the circulating projectiles. The typical areal thickness was 1.3×10^{14} cm^{-2}, which resulted in luminosities of 1×10^{29} to 2×10^{29} cm^{-2} s^{-1}.

The central detector consisted of two 7×8 arrays of CsI(Na) modules on each side of the beam. They constituted electromagnetic calorimeters (CEC, as shown in Fig. 2) with thickness of about 16 radiation lengths and covered an angular range of $30° \leqslant \Theta_{lab} \leqslant 90°$. With respect to the horizontal plane the azimuthal coverage varied with Θ_{lab} from $-25° \leqslant \Phi \leqslant +25°$ (at $\Theta_{lab} = 90°$) to $-40° \leqslant \Phi \leqslant +40°$ (at $\Theta_{lab} = 30°$). Thin scintillator bars (CFB) in front of the CECs allowed to veto charged particles. In addition, there were upstream counters to veto beam halo events.

The forward detector covered scattering angles Θ_{lab} from $4°$ to $22°$ with a sequence of detectors to provide particle identification and particle momentum by position and energy loss measurements. A segmented, thin (3-mm plastic scintillator) window counter (FWC), serving as trigger on charged hadrons, was followed by two sets of thin walled cylindrical drift chambers (FPC) to determine x and y coordinates for tracking, and by a combination of a scintillator hodoscope (FTH) and range hodoscope (FRH).

The FTH consisted of 5-mm-thick scintillators, one layer of 48 radial shaped elements (refered to as FTH3), preceded by two layers with 24 elements, bent as Archimedian spirals

with opposite helicity. They comprised 1104 triangular pixels [16] for particle identification via ΔE, hit multiplicity measurement, and track separation. The four layers of the FRH, each being 11 cm thick, were sufficient to stop deuterons (protons) with kinetic energies up to 400 MeV (300 MeV). The downstream veto (FVH) finally allowed previously stopped particles to be seperated from penetrating charged particles. A more detailed description of the detector is found in Ref. [17].

C. Luminosity measurement

The absolute luminosity was obtained from the simultaneously measured elastic dp scattering at small ($5° \leqslant \Theta_{lab} \leqslant 15°$) scattering angles, as described in detail in Ref. [13]. The forward going deuteron was identified in the FD, and the recoiling proton was detected with silicon strip detectors, placed outside the scattering chamber behind a 0.5-mm stainless steel vacuum window.

The systematic error associated with the luminosity measurement results from the uncertainty of the reference data [18] for elastic pd scattering (8%), and from the scatter of the angular distribution measured with the strips as compared to the reference value, which amounted to 5% (15%) for the second (first) run period. The integrated luminosities are listed in Table I.

D. Triggers

The total event rate in the WASA/PROMICE setup was in the order of 10^5 Hz. A two-level hardware trigger reduced the event rate to less than 1 kHz. The main physics trigger (referred to as TI) selected events with two charged particles stopped in the FRH by requiring two coincident hits in the window counters (FWC), the first two layers of the forward hodoscope (FTH) and no hit in the downstream veto (FVH). The veto condition suppressed breakup events $dp \rightarrow npp$ with energetic protons, without affecting the pion producing channels and $dp \rightarrow dp\gamma$. At the two lowest beam energies of $T_d = 455$ MeV (and $T_d = 437$ MeV) the last (last two) layers of FRH were included as a veto. This did not reduce the acceptance for the pion production channels, for which the experiment was designed, but rejected $dp \rightarrow dp\gamma$ events with proton energies of more than 250 MeV (200 MeV).

In the offline analysis the trigger TI was combined with the request of at least one neutral hit (i.e., no signal in the CFB) with more than 10 MeV deposited in one of the two CsI arrays of the CD. Further, this combination is referred to as trigger TII.

Additional triggers were set up for coincidences of neutral hits in the two parts of the CD for offline identification of the π^0 decay, for light emitting diode generated light pulser events [19] to monitor the detector gains, for the luminosity measurement via elastic dp scattering, and for subevents controlling the FTH, the FRH, the CEC, and the CFB veto detectors offline. These triggers were prescaled for proper adjustment of the trigger rates.
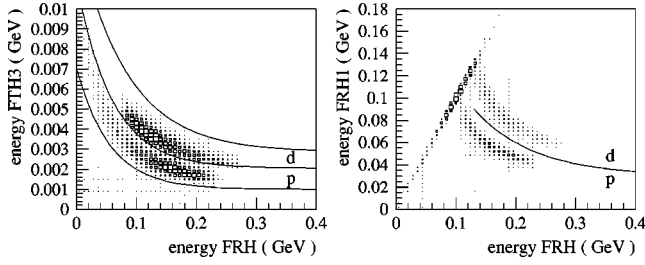
FIG. 3. Cuts used for particle separation with data from events taken at $T_d = 559$ MeV and mainly originating from the $dp \rightarrow dp\pi^0$ reaction.

E. Detector calibration and particle identification

The position dependent energy calibration of the FD plastic scintillators was obtained with dedicated pp elastic scattering runs.

The CsI crystals were calibrated with photons from the $\pi^0 \rightarrow 2\gamma$ decay, where π^0s of precisely known kinetic energy were produced in $pp \rightarrow pp\pi^0$ reactions with two protons in the FD. As a result, the reconstructed π^0 invariant mass $m_{\gamma\gamma}$ showed a width of about 10 MeV (σ).

The particle identification made use of the trigger mode together with hit pattern and pulse height information.

The identification of protons and deuterons in the FD was based on the ΔE-E technique. Since the discrimination of deuterons against the more copious protons was most crucial for our experiment, software cuts were carefully explored by first determining the loci of protons from supplementary measurements of, e.g., $pp \rightarrow pp\pi^0$ and $pp \rightarrow d\pi^+$ events.

Figure 3 shows a good separation obtained between protons and deuterons. Whenever necessary, cuts were set close to the deuterons to minimize misinterpretation of protons. A small fraction of events with deuterons in the exit channel may be lost this way due to the finite energy resolution and the impact of dead detector material.

Inefficiencies of the detector due to secondary interaction losses, in particular, due to breakup reactions of deuterons, have been studied in detail and were taken care of by extension of the GHEISHA code used in the GEANT [20] based Monte Carlo simulations [21,13]. Uncertainties in the reaction probabilities for deuterons led to a total systematic uncertainty of 15% for the deuteron acceptance compared to about 1% for protons.

Photons were detected in the CD only, requiring a hit with at least 10 MeV energy deposited in the CEC crystals and no hit in the corresponding CFB veto. No discrimination against neutrons was applied so they are also classified as neutral hits.

F. Event identification

Similar to the analysis of the $dp \rightarrow dp\pi^0$ reaction [13], events with one identified deuteron and one identified proton have been selected with the TII trigger condition. As an example, Fig. 4(a) shows the squared missing mass distribution of the deuteron-proton pair for the event sample at $T_d = 492$ MeV. Two peaks are clearly visible, one around the squared π^0 mass and one around 0 MeV^2/c^4 originating
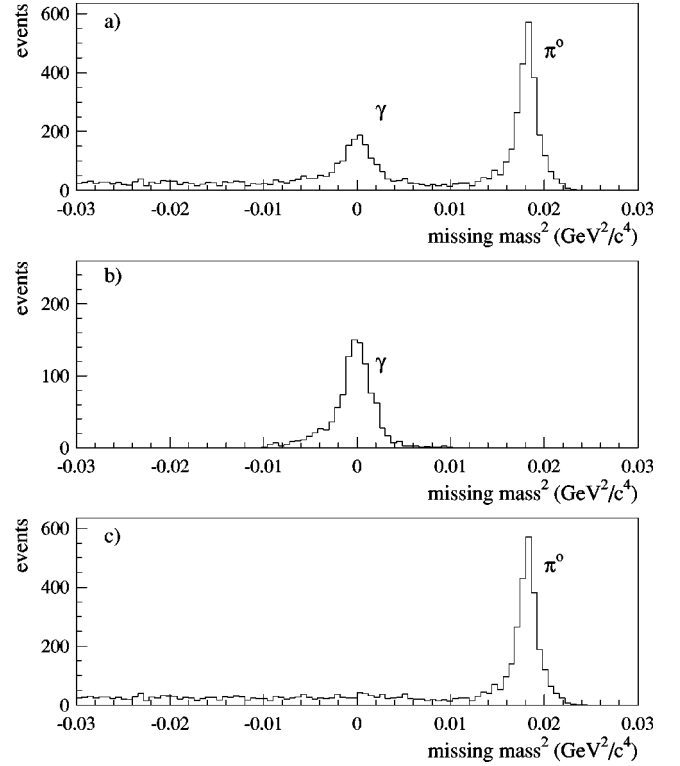
FIG. 4. Squared missing-mass distributions of candidate $dp\gamma$ events at a beam energy of $T_d = 492$ MeV; (a) events obtained under the condition of an identified deuteron and an identified proton plus one neutral hit in the central detector, (b) remaining events under the additional constraint on the γ angle and after a cut on the squared missing mass, and (c) is the complement to (b) and contains the background.

from $dp \rightarrow dp\gamma$. The missing energy of the deuteron-proton pair exceeded always 70 MeV so that elastic dp scattering can safely be excluded.

To select a clean data sample of bremsstrahlungs events, we required a match between the direction of the missing momentum of the deuteron-proton pair and the measured angle of the neutral hit, assuming that it originates from the γ. The difference of the two was required to be less than $23°$ in the laboratory system. In addition, a cut on the squared missing mass (m.m.^{2}) of -0.01 GeV^2/c$^4 \leqslant$ m.m.$^2 \leqslant 0.01$ GeV^2/c^4 has been applied to reject random coincidences from the π^0 production. Figure 4(b) shows the selected event sample after these cuts. Figure 4(c) is the complement to Fig. 4(b) and contains the background. Similar plots are shown in Fig. 5 for all projectile energies under study.

Within the event selection and during the event analysis we did not make use of the γ-energy information obtained with the CEC calorimeter. The reason is that for hits in the outer crystals a part of the γ energy may not be detectable due to the possibility that a part of the electromagnetic shower is lost at the sides of the crystal arrays due to leakage.

Using the energy information would have restricted our analysis to those events where the γ has hit the central 5×6
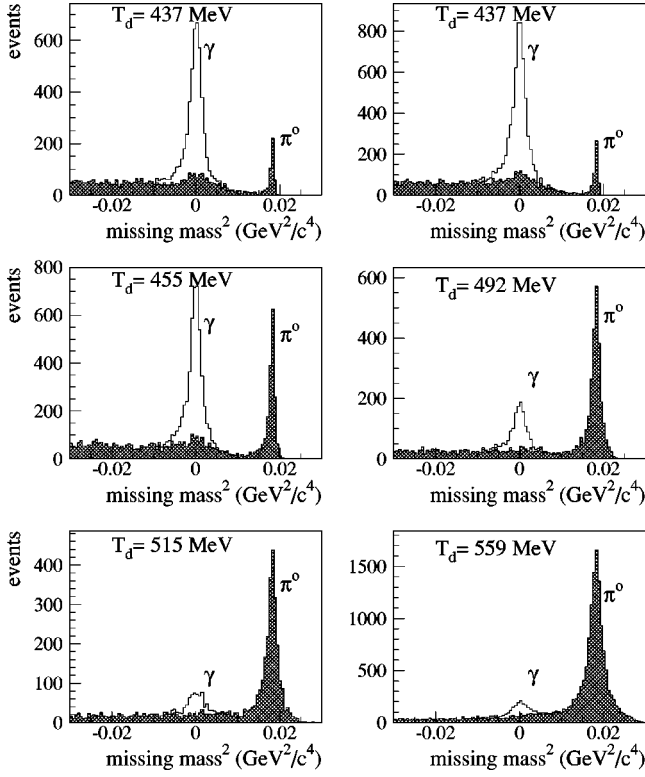
FIG. 5. Squared missing-mass distribution for preselected events for all projectile energies under study. The $dp\gamma$ events (solid lines) are separated from the background (gray areas). The decreasing statistics for the γ events at higher energies reflects only the different integrated luminosities.

out of 7×8 crystals and therefore, reducing our acceptance by nearly a factor of 2.

III. REACTION MODELS AND MONTE CARLO SIMULATIONS

The data analysis presented here follows the principles outlined in Ref. [13] for the analysis of the $dp \to dp\pi^0$ reaction. Apart from quasifree bremsstrahlung off a single nucleon, quantitative microscopic models of reaction mechanisms of bremsstrahlung in $dp \to dp\gamma$ reactions are lacking. Therefore, in our analysis we adopted a more phenomenological approach, attempting to separate the calculable quasifree contribution (3a) from all other reaction mechanisms involving all three nucleons explicitly. For the later coherent production (3b) we used a pure three-body ($dp\gamma$) phase space distribution, characterized by a constant matrixelement. The matrix element used for the quasifree dp bremsstrahlung process that is added incoherently is described in the following.

A. Quasifree bremsstrahlung $pd \to d\gamma p_s$

Meyer and Niskanen [22] have evaluated the $pd \to pd\pi^0$ cross section by relating it to the elementary process $pn \to d\pi^0$. For the pion production close to threshold they calculate the matrix element

$$|M_{pd \to d\pi^0 p_s}|^2 = \frac{2E'_p E'_B E'_s}{E^*_n E^*_p} |\Phi_d(\kappa)|^2 \, |M_{pn \to d\pi^0}|^2. \quad (1)$$

Following their notation, the first factor is a phase space factor that contains total energies of the target proton (p), the beam deuteron (B), and the spectator proton (s) in that $pd \to p_s d\pi^0$ reference frame where the final $d\pi^0$ subsystem is at rest (denoted by a prime), and total energies of the participating nucleons p and n in the center-of-mass (c.m.) system of the $pn \to d\pi^0$ reaction (denoted with an asterisk). The two reference systems differ only slightly due to the fact that the target neutron is bound in the first, but free in the second system. $|\Phi_d(\kappa)|^2$ is the probability density of the neutron momentum $\vec{\kappa}$ in the beam deuteron rest frame calculated from the Bonn potential [23]. Within the initial deuteron rest frame the spectator proton has consequently a momentum $\vec{p}_s = -\vec{\kappa}$.

$|M_{pn \to d\pi^0}|^2$ has been parameterized in terms of the experimentally observed differential cross section for the reaction $pn \to d\pi^0$:

$$|M_{pn \to d\pi^0}|^2 = 16(2\pi)^2 s_2 \frac{p^*_p}{q^*} \frac{d\sigma_{pn \to d\pi^0}}{d\Omega_{q*}}, \quad (2)$$

where s_2 denotes the squared invariant mass of the $pn \to d\pi^0$ system, and p^*_p and q^* are the proton and pion momenta, respectively.

This model succeeded in describing a significant fraction of the $dp \to dp\pi^0$ event yield, which we have observed at those beam energies where all possible neutron momenta within the deuteron could contribute to the pion production [13]. Therefore, it seemed natural to apply this model also to describe the $pd \to d\gamma p_s$ reaction in terms of the quasifree $pn \to d\gamma$ cross section by basically replacing the π^0 with γ.

Applying this change to the quasifree model for $pd \to d\pi^0 p_s$ from now on q^* denotes the momentum of the γ and s_2 the squared invariant mass in the $pn \to d\gamma$ system, and we get from Eqs. (1) and (2) for $pd \to d\gamma p_s$:

$$|M_{pd \to d\gamma p_s}|^2 = \frac{2E'_p E'_B E'_s}{E^*_n E^*_p} |\Phi_d(\kappa)|^2 64\pi^2 s_2 \frac{p^*_p}{q^*} \frac{d\sigma_{pn \to d\gamma}}{d\Omega_{q*}}. \quad (3)$$

Application of Eq. (3) requires the knowledge of the differential cross sections $d\sigma_{pn \to d\gamma}/d\Omega_{q*}$ over a broad range of energies.

These cross sections are, however, not well known. Nicklas *et al.* [27] discuss angular distributions of the neutron induced capture process $np \to d\gamma$ in context with data and theoretical predictions for the inverse process of deuteron photodisintegration. They find substantial differences concerning the absolute values of the cross sections. Their angular distributions showed, besides a flat maximum near $\Theta_{\text{c.m.}} \approx 70°$, no structure.

Based upon a larger set of data, Jenkins *et al.* [24] have parameterized the total and differential cross sections for the photodisintegration process $\gamma d \to pn$ for photon energies be-

tween 20 MeV and 440 MeV. They represented it by the usual Legendre polynomial expansion to fourth order:

$$\frac{d\sigma_{\gamma d \to pn}}{d\Omega_{p*}} = \sum_{l=0}^{4} A_l(E_\gamma) P_l(\cos\Theta^*) \quad (4)$$

with Θ^* being the c.m. angle between the incoming photon and outgoing proton and $A_l(E_\gamma)$ extracted from a pruned data set.

Based on reciprocity, the inverse cross section can then be calculated from

$$\frac{d\sigma_{pn \to d\gamma}}{d\Omega_{q*}} = \frac{9}{4} \frac{p_p^{*2}}{q^{*2}} \frac{d\sigma_{\gamma d \to pn}}{d\Omega_{p*}}, \quad (5)$$

where the squared ratio of center-of-mass momenta for the entrance (p_p^*) and exit (q^*) channel for the same center of mass energy is deduced from kinematics as

$$\frac{p_p^{*2}}{q^{*2}} = \frac{4E_\gamma^2 m_d^2}{[2m_d E_\gamma + m_d^2 - (m_p + m_n)^2][2m_d E_\gamma + m_d^2 - (m_n - m_p)^2]}. \quad (6)$$

B. Monte Carlo simulation

The analysis was accompanied by a complete GEANT based [20] Monte Carlo (MC) simulation. As mentioned above events can be generated either according to phase space or using the quasifree model, i.e., with a weighting proportional to the squared transition matrix elements $|M|^2$ according to Eq. (3).

The MC events were then analyzed with the same method as the experimental data.

C. Decomposition of the quasifree contribution

The experimental observables used in the analysis were the laboratory angles Θ_p, Θ_d and energies T_p, T_d of the dp pairs, as well as their opening angles $\angle_{dp}$ and coplanarities $\Delta\Phi_{dp} = \Phi_d - \Phi_p$. With these six observables the events are kinematically fully determined.

The γ angle has already been used as a constraint for the event selection and, as mentioned earlier, its energy information has not been required throughout the analysis to increase the acceptance of the CEC.

We now base our results on the agreement between the experimental distributions and the distributions of reconstructed, MC generated events.

In order to quantify to which extent the quasifree and the coherent models can reproduce the data, a simultaneous fitting procedure to the six observables has been applied at each projectile energy. This procedure yields (i) the contribution of the two reaction mechanism included in the event generation, (ii) the reaction cross sections, and (iii) the detector efficiency. The same procedure has been used before for the analysis of $dp \to dp\pi^0$ and is described in detail in Ref. [13].

IV. RESULTS AND DISCUSSION

A. Experimental observables

Figure 6 shows the experimental observables at T_d =455 MeV in comparison to a best fit with a quasifree and a coherent contribution. The distributions at the other beam

energies exhibit similar qualitative features and differ only due to statistical uncertainty of the number N_{exp} of observed events (see Table I) and the slightly different detector acceptance.

As a result of the fit procedure, we got the best description of the experimental data with contributions from the quasifree process varying between 57% and 65% in the projectile energy range under study.

The most significant evidences for the quasifree process are the distributions of the assigned spectator protons. These protons can be expected to be emitted with approximately half the deuteron beam momentum folded with the momentum distribution inside the deuteron. Indeed a significant number of protons is emitted at small angles with a peak at half the deuteron beam energy. This is in clear contradiction to what is expected for a pure phase space distributed process.

Nevertheless, the quasifree model fails to explain the excess of protons emitted at larger angles and lower kinetic energies. These events can only be explained assuming that the protons have participated in the reaction mechanism by more than just carrying away their initial momenta. A similar result has been found for the $dp \to dp\pi^0$ channel [13].

Good agreement is seen in the MC description of the other observables as well. However, the experimental energy distributions favor slightly higher deuteron and smaller proton energies. This may be an indication for the presence of an attractive final state interaction between the outgoing deuteron and protons, which has not been included in the MC event generation process for $dp \to dp\gamma$. Inclusion of such a final state interaction has already been proposed in Ref. [22] to explain the $pd \to pd\pi^0$ data of Ref. [25]. However, within the quasifree model such a final state interaction fails to explain the observation of protons under larger angles [13]. Therefore, it seems more reasonable to assign this discrepancy to a poor description of the coherent mechanisms.

It is worth noting that for the $dp \to dp\pi^0$ process the quasifree fraction is small (less than 20%) close to the $3N$ threshold. However, it increased monotonically to about 60% for projectile energies of more than 150 MeV above this
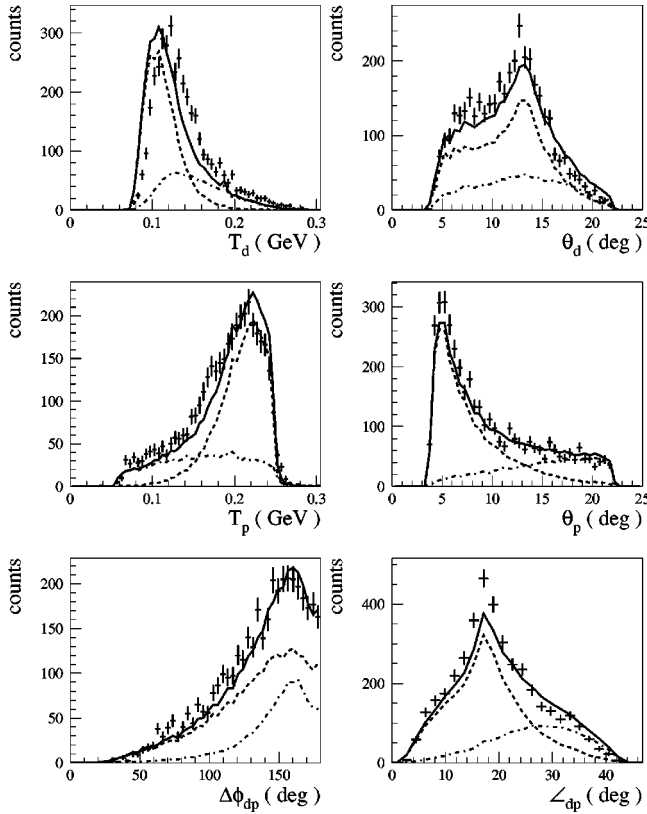
FIG. 6. Experimental angular and energy distributions of the $dp \rightarrow dp\gamma$ observables (crosses) at $T_d = 455$ MeV in comparison to a best fit (solid line) composed of a quasifree (QF, dashed) and a phase space contribution (dash-dotted). The steep fall in the proton energy distribution at about 250 MeV is due to the use of the last layer of FRH as a veto at this beam energy.

FIG. 7. Dalitz plots for $dp \rightarrow dp\gamma$ at $T_d = 492$ MeV. The invariant mass within the $p\gamma$ system is plotted versus the invariant mass within the $d\gamma$ system. The left column shows the whole set of generated events for the two models, while the right column includes the acceptance of the experiment. The first row contains the Monte Carlo data for a pure phase space distribution. The second row shows those events that have been generated assuming the quasifree production process. The plot in the third row contains experimental data.

threshold. Therefore, it was not possible to describe this data without including coherent contributions [13].

From a study of double-pion production in the dp system with deuteron projectile energies from 1.63 GeV to 2.35 GeV, fractions of 40% to 53% for a proton spectator mechanism emerged [26]. This is yet another example that far above thresholds where kinematic constraints on a quasifree process are small, a substantial contribution from mechanisms involving all three nucleons is present.

B. Phase space coverage, detector efficiency

The degree of confidence in the experimental results requires a careful examination of the detector acceptance for the two different models under study.

For the $dp \rightarrow dp\pi^0$ experiment [13] the use of a deuteron beam was crucial to get access to the region of phase space where spectator protons are expected. For pion production the kinematics constrain protons and deuterons to forward angles and the acceptance of the experiment was mainly limited by the beam pipe.

For the $dp \rightarrow dp\gamma$ studies the situation is significantly different. Similar to elastic dp scattering, protons may be emitted up to the maximum angle of close to $\Theta_{lab} = 90°$, but—due to the experimental conditions—they were only detectable up to $\Theta_{lab} = 22°$. In addition, we restricted our

analysis to those events with γ's emitted between $30° < \Theta_{lab} < 90°$ to get clean event samples.

The Dalitz plots in Fig. 7 show the impact of the acceptance for quasifree and for coherent γ production: The experiment was sensitive to approximately half of the phase space covered by the quasifree bremsstrahlung process where the proton is always emitted towards forward angles, but only to a small fraction of the phase space that can be populated by the coherent bremsstrahlung processes.

This can also be translated in terms of the γ energy E_γ. The quasifree model populates the areas of phase space around a constant invariant mass $\sqrt{s_{d\gamma}}$ with a spread given by the Fermi momentum distribution of the spectator proton. Within the beam energy range, under study, this is equivalent to 100 MeV $< E_\gamma <$ 200 MeV for which the detector setup had a good sensitivity, while a coherent process may produce γ's of lower energy.

Based upon the small acceptance and since the coherent reaction mechanisms are not known in detail it is therefore not possible to extract reliable total cross sections for these mechanisms.

For the quasifree process, however, the model assumptions are justified by the agreement between Monte Carlo and the experimental data and therefore, one can extrapolate the measured results to the two regions of phase space that were not covered by the detector.

TABLE I. Total cross sections and error estimates for $dp \to d\gamma p_s$.

T_d (MeV)	L_{int} (nb^{-1})	$N_{expt.}$	$\sigma_{tot, dp \to d\gamma p_s}$ (μb)	$\delta\sigma_N$ (%)	$\delta\sigma_d$ (%)	$\delta\sigma_p$ (%)	$\delta\sigma_L$ (%)	$\delta\sigma_{accept}$ (%)
436.7	25.7	2209	8.7 ± 2.3	2	15	1	10	20
436.7	17.4	1787	11.0 ± 3.3	2	15	1	17	20
454.7	21.4	1761	8.1 ± 2.2	2	15	1	10	20
491.8	15.9	480	12.2 ± 3.7	5	15	1	17	20
514.8	7.1	237	11.8 ± 3.3	6	15	1	10	20
559.0	17.2	590	17.9 ± 5.5	4	15	1	17	20

The number of events where the spectator proton escapes undetected into the beam pipe is determined with high accuracy by its momentum distribution in the projectile deuteron. The number of events with γ's emitted at angles not covered by the CD depends, however, mainly on the differential cross section for the $np \to d\gamma$ reaction. To estimate the uncertainties in the determination of the $dp \to d\gamma p_s$ cross section we made the simplified assumption of an elementary $np \to d\gamma$ cross section, which is constant with energy and angle. The values for the total $dp \to d\gamma p_s$ cross section then increased by less than 20% and therefore, we estimate that the systematical error for the acceptance is less than 20%.

C. Cross sections

Results of the present investigations are given in Table I. The errors for the total cross section include the statistical error ($\delta\sigma_N$), the errors for the detection efficiency of protons ($\delta\sigma_p$) and deuterons ($\delta\sigma_d$), the error in the luminosity ($\delta\sigma_L$), and the estimated error from acceptance caused by the uncertainties in the quasifree spectator model ($\delta\sigma_{accept}$). The errors are assumed to be independent and have been added quadratically.

It is difficult to put our results for the quasifree cross section $\sigma_{tot, dp \to d\gamma p_s}$ in a context with previous measurements due to the uncertainties in the reference data. From the compilation [24] and from Ref. [27] the elementary total cross sections for $np \to d\gamma$ can be expected to be around 15 μb for neutron energies of $T_n = 200$ MeV rising slowly to about 18 μb for $T_n = 300$ MeV.

As a first approximation—where the neutron energies compare to half the deuteron beam energies T_d—our quasifree model results are in a rough agreement of the extracted cross section with the free two nucleon measurements.

For the $pd \to X\gamma$ case there exist some inclusive total cross sections at energies between $T_p = 195$ MeV and 200 MeV just below the pion production threshold [2,5,6], corresponding to about $T_d = 400$ MeV in our case. Consistent values around $\sigma_{tot} = 34$ μb are reported.

Therefore, we conclude from our exclusive data that $dp \to d\gamma p_s$ is one of the most important mechanisms with a contribution of about 30% to the overall bremsstrahlung spectrum in this energy range.

The measurements for $pd \to {}^3$Heγ yielded cross sections that were significantly lower with 1.5 μb at $T_p = 156$ MeV [9] and falling below a 1 μb [10] within the energy range covered by our experiment.

V. SUMMARY AND OUTLOOK

For the first time the reaction $dp \to d\gamma p$ has been studied exclusively in a kinematically complete experiment at five deuteron projectile energies above the pion production threshold. Spectroscopy of the forward going deuterons and protons was performed with the PROMICE/WASA setup. An additional detection of the γ allowed to discriminate background events. Simultaneous measurement of the elastic dp scattering provided the luminosity reference for absolute cross sections.

The detector acceptance covered the quasifree $dp \to d\gamma p_s$ process but was only sensitive to a small fraction of phase space where coherent bremsstrahlung involving all three nucleons can be expected.

Within the covered range of the experiment angular and energy distributions of the outgoing nucleons showed characteristics that can be predicted assuming an elementary $np \to d\gamma$ process with a spectator proton. However, the spectroscopy of the outgoing protons indicated also the presence of other processes involving all three nucleons similar to previous measurements of the meson production reaction $dp \to dp\pi^0$ [13].

Exclusive cross sections are given for the $dp \to d\gamma p_s$ process, showing that this reaction mechanism plays an important role in pd bremsstrahlung.

With $dp \to {}^3$Heγ reaction contributing only a small fraction of the total pd bremsstrahlung it would be interesting to also measure exclusive data for all the other competing reaction mechanisms with a large acceptance in phase space. The use of deuteron projectiles has in this respect proven to be well suited to examine processes with spectator protons and to disentangle the exit channels with more than two particles.

[1] M. Kwato *et al.*, Phys. Lett. B **207**, 269 (1988).
[2] P.F. Koehler *et al.*, Phys. Rev. Lett. **18**, 933 (1967).
[3] M.A. Pickar *et al.*, Phys. Rev. C **35**, 37 (1987).
[4] K. Nakayama, Phys. Rev. C **45**, 2039 (1992).
[5] J.A. Pinston *et al.*, Phys. Lett. B **249**, 402 (1990).
[6] J. Clayton *et al.*, Phys. Rev. C **45**, 1810 (1992).
[7] H. Huisman *et al.*, Phys. Rev. Lett. **83**, 4017 (1999).
[8] J.A. Edgington and B. Rose, Nucl. Phys. **89**, 523 (1966).
[9] J.P. Didelez *et al.*, Nucl. Phys. **A143**, 602 (1970).
[10] J.M. Cameron *et al.*, Nucl. Phys. **A424**, 549 (1984).
[11] N. Kalantar-Nayestanski, Nucl. Phys. **A631**, 242c (1998).
[12] R. Bilger *et al.*, Nucl. Instrum. Methods Phys. Res. A **457**, 64 (2001).
[13] J. Greiff *et al.*, Phys. Rev. C **62**, 064002 (2000).
[14] H. Calén *et al.*, Phys. Rev. Lett. **79**, 2642 (1997).
[15] C. Ekström, Nucl. Instrum. Methods Phys. Res. A **362**, 1 (1995).
[16] M. Dahmen *et al.*, Nucl. Instrum. Methods Phys. Res. A **348**, 97 (1994).
[17] H. Calén *et al.*, Nucl. Instrum. Methods Phys. Res. A **379**, 57 (1996).
[18] H. Rohdjeß *et al.*, Phys. Rev. C **57**, 2111 (1998).
[19] J. Zabierowski, Nucl. Instrum. Methods Phys. Res. A **383**, 577 (1994).
[20] CERN Program Library Long Writeup W5013.
[21] J. Greiff, Ph.D. thesis, Universität Hamburg, Hamburg, 1999.
[22] H.O. Meyer and J.A. Niskanen, Phys. Rev. C **47**, 2474 (1993).
[23] R. Machleidt, K. Holinde, and C. Elster, Phys. Rep. **149**, 66 (1987).
[24] D.A. Jenkins *et al.*, Phys. Rev. C **50**, 74 (1994).
[25] H. Rohdjeß *et al.*, Phys. Rev. Lett. **70**, 2864 (1993).
[26] T. Tsuboyama *et al.*, Phys. Rev. C **62**, 034001 (2000).
[27] G. Nicklas *et al.*, Phys. Lett. **141B**, 170 (1984).